Research Article | Vol. 6, No. 11 | 1 Nov 2016 | OPTICAL MATERIALS EXPRESS 3455

Optical Materials EXPRESS

Dimensional changes in slanted diffraction gratings recorded in photopolymers

R. FERNÁNDEZ,[1] S. GALLEGO,[1,2,*] V. NAVARRO-FUSTER,[1,2] C. NEIPP,[1,2] J. FRANCÉS,[1,2] S. FENOLL,[1,3] I. PASCUAL,[1,2] AND A. BELÉNDEZ[1,2]

[1]*Instituto Universitario de Física Aplicada a las Ciencias y las Tecnologías, Universidad de Alicante, Apartado 99, 03080 Alicante, Spain*
[2]*Departamento de Física, Ingeniería de Sistemas y Teoría de la Señal, Universidad de Alicante, Apartado 99, E03080 Alicante, Spain*
[3]*Departamento de Óptica, Farmacología y Anatomía, Universidad de Alicante, Apartado 99, E03080 Alicante, Spain*
**sergi.gallego@ua.es*

Abstract: Photopolymers are appealing materials for many optical applications. For most of them, shrinkage plays an important role in the final properties of the display, especially in holographic data storage applications. In this paper, we demonstrate that to quantify correctly the shrinkage, it is mandatory to measure the angle of propagation for both diffracted orders ± 1, so that an accurate value of the grating vector can be calculated. Experimental evidence from three different photopolymers supports this affirmation. Firstly, polyvinyl alcohol acrylamide based photopolymer, which has been studied by many research groups; secondly, one environmentally compatible photopolymer developed by our group; and thirdly, a photopolymer with dispersed liquid crystal molecules. We studied the deviation from the sinusoidal profile analyzing the higher diffracted orders.

OCIS codes: (050.0050) Diffraction and gratings; (160.5335) Photosensitive materials.

References and links

1. M. Infusino, A. De Luca, V. Barna, R. Caputo, and C. Umeton, "Periodic and aperiodic liquid crystal-polymer composite structures realized via spatial light modulator direct holography," Opt. Express **20**(21), 23138–23143 (2012).
2. E. Tolstik, O. Romanov, V. Matusevich, A. Tolstik, and R. Kowarschik, "Formation of self-trapping waveguides in bulk PMMA media doped with Phenanthrenequinone," Opt. Express **22**(3), 3228–3233 (2014).
3. H. Li, Y. Qi, J. P. Ryle, and J. T. Sheridan, "Self-written waveguides in a dry acrylamide/polyvinyl alcohol photopolymer material," Appl. Opt. **53**(34), 8086–8094 (2014).
4. E. Leite, I. Naydenova, S. Mintova, L. Leclercq, and V. Toal, "Photopolymerizable nanocomposites for holographic recording and sensor application," Appl. Opt. **49**(19), 3652–3660 (2010).
5. A. C. Urness, K. Anderson, C. Ye, W. L. Wilson, and R. R. McLeod, "Arbitrary GRIN component fabrication in optically driven diffusive photopolymers," Opt. Express **23**(1), 264–273 (2015).
6. R. Fernández, S. Gallego, A. Márquez, J. Francés, V. Navarro-Fuster, and I. Pascual, "Diffractive lenses recorded in absorbent photopolymers," Opt. Express **24**(2), 1559–1572 (2016).
7. H. J. Coufal, D. Psaltis, and G. T. Sincerbox, eds., *Holographic Data Storage* (Springer–Verlag, 2000).
8. K. Curtis, L. Dhar, A. Hill, W. Wilson, and M. Ayres, eds., *Holographic Data Storage: From Theory to Practical Systems* (John Wiley & Sons, Ltd, 2010).
9. M. P. Jordan and L. Solymar, "A note on volume holograms," Electron. Lett. **14**(9), 271–272 (1978).
10. J. T. Gallo and C. M. Verber, "Model for the effects of material shrinkage on volume holograms," Appl. Opt. **33**(29), 6797–6804 (1994).
11. J. H. Chen, D.-C. Su, and J.-C. Su, "Shrinkage- and refractive-index shift-corrected volume holograms for optical interconnects," Appl. Phys. Lett. **81**(8), 1387–1389 (2002).
12. S. H. Stevenson ; K. W. Steijn; Method for characterization of film thickness and refractive index in volume holographic materials. Proc. SPIE 2405, Holographic Materials, 88 (March 23, 1995).
13. C. Zhao, J. Liu, Z. Fu, and R. T. Chen, "Shrinkage correction of volume phase holograms for optical interconnects. Proc. SPIE 3005," Optoelectronic Interconnects and Packaging **IV**, 224–229 (1997).
14. G. Ramos, A. Álvarez-Herrero, T. Belenguer, F. del Monte, and D. Levy, "Shrinkage control in a photopolymerizable hybrid solgel material for holographic recording," Appl. Opt. **43**(20), 4018–4024 (2004).
15. M. Moothanchery, I. Naydenova, and V. Toal, "Study of the shrinkage caused by holographic grating formation in acrylamide based photopolymer film," Opt. Express **19**(14), 13395–13404 (2011).

#268022 http://dx.doi.org/10.1364/OME.6.003455
Journal © 2016 Received 10 Jun 2016; revised 16 Sep 2016; accepted 16 Sep 2016; published 6 Oct 2016

Optical Materials EXPRESS

16. T. Sabel and M. Zschocher, "Imaging of Volume Phase Gratings in a Photosensitive Polymer, Recorded in Transmission and Reflection Geometry," Appl. Sci. **4**(1), 19–27 (2014).
17. L. Dhar, M. G. Schnoes, T. L. Wysocki, H. Bair, M. Schilling, and C. Boyd, "Temperature-induced changes in photopolymer volume holograms," Appl. Phys. Lett. **73**(10), 1337–1339 (1998).
18. E. Hata and Y. Tomita, "Order-of-magnitude polymerization-shrinkage suppression of volume gratings recorded in nanoparticle-polymer composites," Opt. Lett. **35**(3), 396–398 (2010).
19. P. Vojtíšek, M. Květoň, and I. Richter, "Complex method for angular-spectral analysis of volume phase diffraction gratings recorded in photopolymers," Journal of the European Optical Society - Rapid publications," Europe **11** (2016).
20. N. Pandey, I. Naydenova, S. Martin, and V. Toal, "Technique for characterization of dimensional changes in slanted holographic gratings by monitoring the angular selectivity profile," Opt. Lett. **33**(17), 1981–1983 (2008).
21. S. Gallego, A. Márquez, D. Méndez, C. Neipp, M. Ortuño, M. Alvarez, E. Fernandez, and A. Beléndez, "Real-time interferometric characterization of a polyvinyl alcohol based photopolymer at the zero spatial frequency limit," Appl. Opt. **46**(30), 7506–7512 (2007).
22. M. Moothanchery, V. Bavigadda, V. Toal, and I. Naydenova, "Shrinkage during holographic recording in photopolymer films determined by holographic interferometry," Appl. Opt. **52**(35), 8519–8527 (2013).
23. M. Kawana, J. Takahashi, J. Guo, and Y. Tomita, "Measurement of polymerization-shrinkage evolution during curing in photopolymer with a white-light Fabry-Pérot interferometer," Opt. Express **23**(12), 15356–15364 (2015).
24. T. Sabel, "Spatially Resolved Analysis of Bragg Selectivity," Appl. Sci. **5**(4), 1064–1075 (2015).
25. C. Neipp, A. Beléndez, S. Gallego, M. Ortuño, I. Pascual, J. Sheridan, and J. T. Sheridan, "Angular responses of the first and second diffracted orders in transmission diffraction grating recorded on photopolymer material," Opt. Express **11**(16), 1835–1843 (2003).
26. V. Navarro-Fuster, M. Ortuño, S. Gallego, A. Márquez, A. Beléndez, and I. Pascual, "Biophotopol's energetic sensitivity improved in 300 μm layers by tuning the recording wavelength," Opt. Mater. **52**, 111–115 (2016).
27. S. Gallego, M. Ortuño, A. Márquez, R. Fernández, M. Álvarez, I. Pascual, A. Beléndez, "Influence of Thickness on the Holographic Parameters of H-PDLC Materials," International Journal of Polymer Science **2014**, 528287 (2014).
28. C. E. Close, M. R. Gleeson, and J. T. Sheridan, "Monomer diffusion rates in photopolymer material. Part I. Low spatial frequency holographic gratings," J. Opt. Soc. Am. B **28**(4), 658–666 (2011).
29. Y. J. Liu and X. W. Sun, "Holographic polymer-dispersed liquid crystals: Materials, formation, and applications," Advances in OptoElectronics **2008**, 684349 (2008).
30. H. Kogelnik, "Coupled wave theory for thick hologram gratings," Bell Syst. Tech. J. **48**(9), 2909–2947 (1969).
31. M. G. Moharam and T. K. Gaylord, "Rigorous coupled-wave analysis of planar-grating diffraction," J. Opt. Soc. Am. **71**(7), 811–818 (1981).
32. J. Francés, S. Bleda, C. Neipp, A. Márquez, I. Pascual, and A. Beléndez, "Performance analysis of the FDTD method applied to holographic volume gratings: Multi-core CPU versus GPU computing," Comput. Phys. Commun. **184**(3), 469–479 (2013).
33. S. Gallego, M. Ortuño, I. Pascual, C. Neipp, A. Márquez, and A. Beléndez, "Analysis of Second and Third Diffracted Orders in Volume Diffraction Gratings Recorded on Photopolymers," Phys. Scr. T **2005**, T118(2005).

1. Introduction

Thick recording materials such as photopolymers can be adapted for many different optical applications, every day new perspectives are proposed in fields like photonic structures [1], waveguides [2,3], sensors [4], or diffractive lenses [5,6]. Photopolymers are versatile and appealing optical recording materials due to their dynamical chemical composition, the possibility of introducing many new components and their low cost. Initially the photopolymeric formulations were designed for holography, in particular, due to their property for fabricating thick layers, of more than 500 μm, proposed as a base of holographic data memories [7,8]. In this sense, many efforts have been done in this field. Some technological companies have focused their attention on optimizing photopolymers for holographic data storage applications, where the recording material is the key to obtain a final competitive product.

There are some criteria for the recording material to be used in a holographic data storage application. Some of them are the material sensitivity, between of 100-1000 mJ/cm^2 to achieve full dynamic range; refractive index modulation, minimum of $5x10^{-3}$; and shrinkage, maximum of 0.5% [7]. In general it is assumed that shrinkage occurs after the gratings are formed. The assumption that one side of the material is attached to a rigid substrate is the basis of the fringe rotation model [9], this can be a reminiscence of the initial steps of the holography where silver halide emulsion was the most popular holographic recording material

Optical Materials EXPRESS

[10]. On the other hand, in general a common approach to modelling Bragg shift in replay properties it is to assume negligible refractive index change [11]. Measuring where the Bragg's condition is located to achieve maximum diffraction efficiency in the reconstruction scheme is the standard method to measure shrinkage. The values provided by this technique sometimes slightly differ from results provided by mechanical systems; some authors suggested that this difference in optical measured shrinkage is the effect of the average refractive-index change [12]. The method most referenced in order to measure the holographic shrinkage was devolved by Z. Zhao et al [13]. This work provided very useful explicit equations to relate the shrinkage with the variation of the spatial period of the recorded gratings and was used by some authors [14–16]. The geometrical approximation proposed in ref. 13 is reproduced schematically in Fig. 1. In this figure the recorded fringes are represented by continues lines and separated by a spatial period Λ. The fringes after shrinkage are represented by discontinues lines and separated by a new period Λ'. K is the grating vector; ρ and σ are the propagation vectors of the recording beams inside the recording material; d is the initial thickness and d' the thickness after shrinkage; L is the maximum length of the fringes and Λx and Lx are two constants independent of the shrinkage and derived from the assumed conservation of the x component of K, Kx in this model.

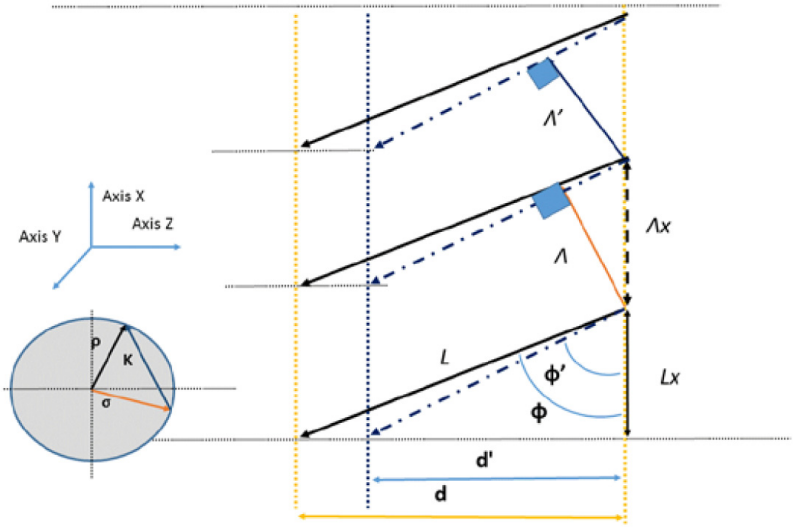

Fig. 1. Model of shrinkage proposed in [12]. Light travels to the positive direction of axis Z. The Ewald's sphere.

Following the diagram represented in Fig. 1 these two expressions can be obtained:

$$\Lambda' = \Lambda \frac{\sin(\phi')}{\sin(\phi)}. \tag{1}$$

$$d' = d \frac{\tan(\phi')}{\tan(\phi)} \tag{2}$$

Additionally, at the same time, very similar analysis and equations to determine shrinkage from Bragg's angle detuning were used by L. Dhar [17], and more recently this analysis was applied to study the shrinkage suppression due to the nanoparticles inclusion in photopolymers [18]. Nevertheless, nowadays choosing a method to measure the amount of the shrinkage in holographic recording materials can still be considered a hot topic. This year it has been published an interesting work that report a complete analysis of the problem

Optical Materials EXPRESS

combining the Bragg's angle detuning and Bragg's wavelength detuning, using the Kogelnik's wave coupled theory, KCW, and the rigorous analysis, RCW, proposed by Moharam et al. [19].

Nowadays new alternative techniques have been proposed in order to measure the shrinkage in photopolymers [20–23] and the influence of different parameters on the changes observed in the spatial period [24]. These alternative methods to the holographic Bragg-angle detuning measurements provide information of the material shrinkage in real time. The first of them consists in the measurements of the diffraction pattern of a probe divergent beam [25] obtaining values less than 0.75% for polyvinyl alcohol acrylamide (PVA/AA) photopolymer, recording intensity of 5 mW/cm^2 and spatial frequency 600 lines/mm. This result is slightly lower than the measured in ref [14]. by Bragg's angle detuning method assuming the conservation of Kx, 1% for spatial frequencies of 600 lines/mm and around 1.2% for 1000 lines/mm, furthermore for lower recording intensities, 1 mW/cm^2, the shrinkage increases from 1.2 to 2%. It is interesting to notice that the original method based on holographic interferometry provides shrinkage values also in real time [22]. It is worth remarking that with this last method the obtained values of shrinkage are around 3% for similar holographic gratings and exposure times (100s). It seems very elevated, attending to the assumed model where the shrinkage is produced by polymerization in the illuminated zones, and is partially suppressed by the monomer migration, described by Fick's law, from dark zones to bright ones. In this sense, it is important to note that the highest limit of shrinkage due to polymerization in PVA/AA materials can be obtained using zero-frequency measurements [21], where the diffusion does not take place. The published results indicate that the shrinkage upper limit is 3% for PVA/AA materials without crosslinker and 4% for one with N,N'-methylene-bis-acrylamide (BMA) as crosslinking monomer.

As we commented before, one of the most studied photopolymers is the one based on polyvinyl alcohol acrylamide (PVA/AA) [19–21,24]. Along this work, we have analysed three different types of photopolymers, firstly PVA/AA and secondly one of the greenest photopolymers whose patent belongs to the Alicante University called Biophotopol [26] and on the last place a holographic-dispersed liquid crystal photopolymer (H-PDLC) [27]. We have measured the shrinkage and the higher diffracted orders; we have also studied the conservation of the x component of the grating vector, K, for different recording times. We have magnified the error by only taking into account the first Bragg's angle detuning. Following the evidences that the component Kx is not conserved, we study possible deformations in the sinusoidal profile measuring second and third diffracted orders. Additionally, we have proposed an alternative method to obtain the amount of shrinkage for holographic materials.

2. Theoretical background

It is worth noting that the grating vector, **K**, can be obtained easily from the two interfering wave vectors, **ρ** and **σ**, as follows:

$$\boldsymbol{\rho} - \boldsymbol{\sigma} = K \tag{3}$$

where $|\boldsymbol{K}| = \frac{2\pi}{\Lambda}$ and $|\boldsymbol{\rho}| = |\boldsymbol{\sigma}| = n\frac{2\pi}{\lambda}$, Λ is the grating period, λ is the wavelength and n is the average refractive index of the sample.

From Fig. 1 we can obtain these two relations:

$$\frac{\Lambda}{\Lambda_x} = sin(\phi). \tag{4}$$

Optical Materials EXPRESS

$$\frac{d}{L_x} = \tan(\phi) \tag{5}$$

Differencing 4 and 5 and assuming that the changes in Lx and Λx are very small in comparison to the Φ and Λ ones, we can obtain the next two equations:

$$\Delta\Lambda = \Lambda_x \cos(\phi)\Delta\phi \tag{6}$$

$$\Delta d = L_x \frac{1}{(\cos(\phi))^2}\Delta\phi \tag{7}$$

Combining (6) and (7) and substituting the values of Lx and Λx from Eq. (4) and (5) we obtain:

$$\frac{\Delta\Lambda}{\Lambda} = (\cos(\phi))^2 \frac{\Delta d^\circ}{d} \tag{8}$$

where Δd is the shrinkage and ΔΛ is the variation of the period. The initial period is obtained from the two interference beams angles, and to obtain the period after the holographic grating recording there are two ways. Either assuming that the component Kx remains constant and measuring only the + 1 Bragg's angle or taking into account + 1 and −1 diffracted order angles and re-calculating the whole grating vector. An alternative method consists in obtaining the period from the Bragg's condition; in general, Bragg's condition can be obtained from the next equation:

$$\frac{2n}{\lambda}\sin(\theta) = \frac{1}{\Lambda}. \tag{9}$$

where θ is the angle between the replay vector and the fringes. As usually after shrinkage it is difficult to precise the slanted angles of the fringes, it is possible to use an alternative way where Bragg's condition is expressed as a function of the angle formed by **ρ** and **σ** inside the material, φ, as follows:

$$\frac{2n}{\lambda}\sin(\varphi/2) = \frac{1}{\Lambda}. \tag{10}$$

and here we have to measure the two Bragg's angles, corresponding to + 1 and −1 diffracted orders.

3. Experimental

In this work we use three different photopolymers. The first one, PVA/AA is composed by acrylamide (AA) as polymerizable monomer, N,N'-methylene-bis-acrylamide (BMA) as crosslinking monomer, triethanolamine (TEA) as coinitiator and plasticizer, yellowish eosin (YE) as dye, polyvinyl alcohol (PVA) as binder and a small proportion of water as additional plasticizer. Different types of PVA can be used as binder. In this work we have used a PVA 18-88 with Mw = 180000 amu. The particular concentration used in this work is presented in Table 1.

For the preparation of the layer, 30 ml of solution with water as the solvent is deposited using the force of gravity on a glass substrate (25 cm x 20 cm) and left in the dark (RH = 40–45%, T = 20–23 °C). When part of the water has evaporated (after about 36 hours), the layer has enough mechanical resistance and can be cut without deforming. The final "solid" film has a physical thickness around 75 ± 5 μm. This final thickness can be modified changing the quantity of the syrup deposited on the glass, in this work we have studied thicknesses between

Optical Materials EXPRESS

55 and 80 μm with similar results in the shrinkage. We measure the refractive index before exposure using a refractometer; this is 1.4811.

Table 1. Composition of the liquid solution for photopolymer AA.

TEA (ml)	PVA (ml) (8% w/v)	AA (gr)	BMA (gr)	YE (0.8% w/v) (ml)
2.0	25	0.84	0.25	0.7

We analyzed on second place Biophotopol, a high environmental photopolymer [26]. We present its composition in Table 3 with water as solvent, it is composed of sodium acrylate (AONa) as polymerizable monomer, triethanolamine (TEA) as coinitiator and plasticizer, sodium salt 5′-riboflavin monophosphate (PRF) as dye and polyvinyl alcohol (PVA) as binder (Mw = 130000 u, hydrolysis degree = 87.7%). A high TEA content is necessary to plasticize the layer and therefore the water/TEA fraction in this polymer formulation is low. The composition of the photopolymer solution is deposited in circular glass molds by gravity. Initially the liquid solution has around 1450 μm thickness. The molds are then left inside an incubator (Climacell 111) with controlled humidity and temperature (Hr = 60 ± 5% and T = 22 ± 1 °C, respectively). When part of the water has evaporated (40 h), the "solid" film thickness decreases to 300 ± 10 μm. At this time, the layer has enough mechanical resistance and it can be extracted from the mold without deformation. Then, the solid film is cut into 6.5x6.5 cm^2 pieces and adhered to the surface of glass plates without the need of adhesives. The plates are then ready for exposure, which takes place immediately. In this case, the refractive index of the "solid" layer before exposure is 1.4730.

Table 2. Composition of the liquid solution for photopolymer AA.

PVA (% w/v)	AONa (M)	TEA (M)	PRF (M)
15	0.34	0.15	$1.00 \cdot 10^{-3}$

On the last place, the photopolymer with liquid crystal molecules is prepared using the following components: the monomer used is dipentaerythritol penta/hexa-acrylate (DPHPA) with a refractive index n = 1.490. We use the nematic liquid crystal, licristal BL036 from Merck. It is a mixture of 4-cyanobiphenyls with alkyl chains of different lengths. It has an ordinary refractive index n_0 = 1.5270, and a difference between extraordinary and ordinary index Δn = 0.2670 [26]. There is a difference of 0.037 between the ordinary refractive index of the liquid crystal and that of the monomer. The liquid crystal concentration was set at 28 wt% as the starting point for component optimization and remained practically unchanged during this process. N-vinyl-2-pyrrolidone (NVP) was used as crosslinker, N-phenyl glicine (NPG) as radical generator and octanoic acid (OA) as cosolvent [26]. We used ethyl eosin (YEt) as dye.

The H-PDLC prepolymer solution is made by mixing the components under red light at which the material is not sensitive. The solution is sonicated in an ultrasonic bath, deposited between two conductive ITO glass plates of 1 mm thick and separated using two types of glass microspheres. The microspheres were provided by Whitehouse scientific with a thickness between 15 and 20 μm. In this work we used the chemical compositions represented in Table 2. For this syrup the refractive index before polymerization is 1.5225.

Table 3. Composition of photopolymer H-PDLC in wt%

photopolymer	DPHPA	BL036	YEt	NPG	NVP	OA
H-PDLC	48.4	29.2	0.1	1.5	16.4	4.4

The experimental device is a typical transmission holographic set-up; we have represented it in Fig. 2. Nevertheless, due to the different band absorption of the dyes, the recording wavelength must be modified for Biophotopol. For PVA/AA and H-PDLC a Nd:YAG laser

Optical Materials EXPRESS

tuned at a wavelength of 532 nm was used to record diffraction gratings by means of continuous laser exposure. The laser beam was split into two secondary beams with an intensity ratio of 1:1. The diameter of these beams was increased to 1 cm using a spatial filter and collimating lens, while spatial filtering was ensured. The object and reference beams were recombined at the sample at an angle of 15.8 degrees to the normal with an appropriate set of mirrors, and the spatial frequency obtained was 1024 lines/mm for non-slanted gratings. The working intensity at 532 nm was 3 mW/cm^2, this recording intensity is the same for all the photopolymeric materials. We monitored the diffraction grating using red light (λ = 633 nm) at which the dyes do not absorb. After recording, when the green laser was shut off, we rotated the sample to record the angular response around the different Bragg conditions, ± 1, ± 2. Fitting the angular response with different theories, we obtained the data necessary to calculate optical thickness of the holographic diffraction gratings and the value of the grating vector to deduce the shrinkage. To record slanted gratings, we rotated the sample 15°, that means a new spatial frequency depending on the refractive index of material. For PVA/AA with these recording and read out parameters, we obtain 1004 lines/mm, and a Kx = 6.21μm^{-1}. Due to the different refractive index for HPDLC we obtain just a small variation in the spatial frequency, now is 1003 lines/mm

In the case of Biophotopol we use a wavelength of 488 nm, where the dye presents good absorption and the material has higher repeatability. For symmetrical case, non-slanted, both recording beams impinge with an angle of 17.1° [25], once we rotate the stage 15° the spatial frequency is 1182 lines/mm and the initial value of Kx is 7.314 μm^{-1}. For this higher spatial frequency we expect an increase of 40-50% shrinkage value from the obtained at 1004 lines/mm as were reported in [15] for PVA/AA photopolymer.

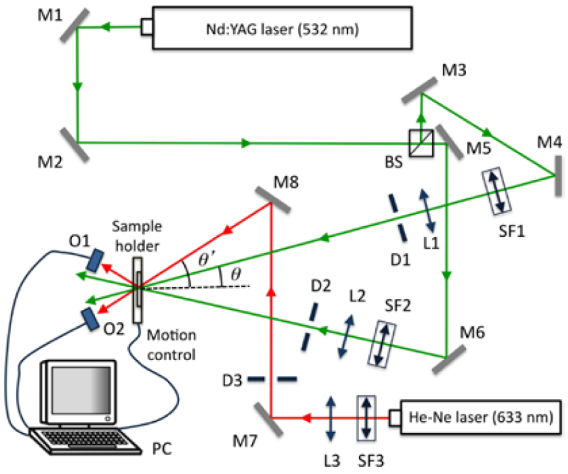

Fig. 2. Experimental set-up. BS: Beamsplitter, Mi: mirror, SFi: spatial filter, Li: lens, Di: diaphragm, Oi: optical power meter, PC: data recorder.

4. Results and discussion

In this section, we present the results obtained from different photopolymers. Along this paper, we present different goals. Firstly, we analyzed the conservation of Kx during the recording process. Then, we calculated the shrinkage for the three different photopolymers comparing also the three methods to measure the shrinkage. On the last place, we seek for possible deformations in the sinusoidal gratings due to shrinkage analyzing higher harmonics, simultaneously we compared different electromagnetic methods to fit the angular responses of the diffracted orders coming out of the gratings, obtaining the optical thicknesses and refractive index modulations.

Optical Materials EXPRESS

4.1. Shrinkage in PVA/AA materials

As we noted in the introduction PVA/AA photopolymer is one of the most studied holographic recording materials. In this point, we want to analyze the diffraction efficiency, DE, and transmission efficiency, TE, versus recording time for a grating recorded in PVA/AA. This information is difficult to obtain in real time for thick slanted gratings, due to their high angular selectivity and the detuning of the Bragg's condition. For example, for a 70 μm thick transmission grating recorded using the experimental set-up described in the last section with maximum diffraction efficiency, DE, drops to 50% when the detuning is around 0.5° in air. In our experiments, the changes in the Bragg's angles are as maximum of 0.4°. Therefore, in order to obtain information about the DE at Bragg's condition as a function of exposure we can record many gratings with different exposure times and measure the maximum DE of each one like the experiments made for holograms recorded in photographic emulsions or situate the readout laser just at the angle where the maximum DE for long time recorded gratings is located. We have selected this possibility in order to show the maximum DE achieved for these holograms. It is important to note that all the DEs presented in this paper are calculated with respect to the incident light. Therefore, due to the Fresnel losses, the maximum DE depends on the diffracted angle, and in all the cases is lower than 92.5%. The results are presented in Fig. 3 for the diffracted order situated around 3.7° in air. We show how the DE achieves a value higher than 80%, very close to the maximum possible for this angle, which shows the good possibilities to record slanted gratings in this material in order to multiplex many gratings such as using angular peristrophic multiplexing.

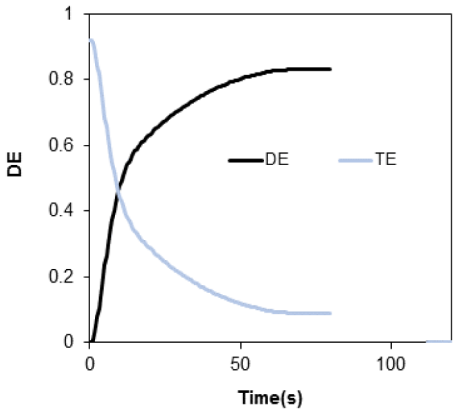

Fig. 3. DE as function of recording time for PVA/AA photopolymer 73 μm thick at Bragg's angle.

Once we have recorded the grating, we measure the Bragg's angles of the orders ± 1, to obtain the value of K and to check possible variations of Kx component. In order to measure possible deviations from the sinusoidal profile of the gratings, we measured the second and third diffracted orders at second and third Bragg's angles respectively [19,25], this will be analyzed in the next section 4.4. We control the initial Bragg's angles in air for the diffracted orders ± 1, and we measured the new ones with an error of ± 0.002°, this accuracy give us an error of 0.09% in the determination of the shrinkage. Nevertheless, we have to add additional imprecisions, firstly measuring the refractive index of the layer with an Abbe refractometer, n = 1.4811 ± 0.0005, secondly, possible average changes in n of 0.003 due to polymerization, and thirdly, the repeatability that implies a total error in the shrinkage of 0.14%. We have presented the measured angles in air for PVA/AA gratings in Table 4. From the analysis of Table 4, we want to remark that while the modulus of K increases with the shrinkage during grating formation, Kx decreases for long recording times for PVA/AA photopolymer. Initially the value of Kx is 6.21 μm^{-1} and measuring Bragg's angles of orders + 1 and −1 we detected

Optical Materials EXPRESS

that, after 80s of recording, this value drops to 6.15 μm^{-1}. This change means an error determining the shrinkage with only one Bragg's angle around ± 2%, the same value of the highest values reported in this paper, in other words, the relative error, measuring only one Bragg's detuning angle, can be higher than 100%. Nevertheless, our results are in consonance with the ones presented in ref [15], where they obtained 2% for recording intensity of 1 mW/cm^2 and 1.2% for 1 mW/cm^2.

Table 4. Measured angular positions in air of the diffracted orders ± 1 and the value of Kx.

Recording time (s)	Angle order + 1 (°)	Angle order −1(°)	Kx (μm^{-1}) ± 0.01
5	3.750	−34.050	6.21
10	3.740	−34.077	6.21
20	3.670	−33.999	6.19
30	3.644	−33.994	6.18
40	3.564	−33.955	6.16
50	3.481	−33.792	6.13
80	3.322	−34.001	6.13

Besides the measured angles, we can calculate the shrinkage following different methods. In this paper we propose to compare three of them, the first one, method 1, is to follow the equation presented by Zhao [13], Eq. (2), obtaining the value of K from the angles of the both first orders, ± 1. The second one, method 2, is using the same equation but assuming the conservation of Kx and deducing the Bragg's condition detuning of the order + 1. On the last place, method 3 is based on the Eq. (8) where the value of the new spatial period is obtained using Bragg's angles of orders ± 1. In Table 5 we present the results provided by the three methods for the same gratings. As it can be seen, method 1 and method 3 provide similar results, only differing in 0.01 at a recording time of 80s. As we mentioned in our hypothesis in the introduction, method 2 seems inconsistent to fit the shrinkage in this material. We want to remark that the shrinkage continues growing even when the DE looks constant.

Table 5. Measured shrinkage using the three methods.

Recording time (s)	% Shrinkage method 1 ± 0.14	% Shrinkage method 2 ± 0.14	% Shrinkage method 3 ± 0.14
5	0.05	0.70	0.02
10	0.08	0.07	0.08
20	0.05	0.00	0.10
30	0.17	0.00	0.17
40	0.29	0.80	0.29
50	0.62	0.67	0.62
80	1.31	0.35	1.30

4.2. Shrinkage in biophotopol

As we have explained in the experimental section, the fabricated layers of this material have an optical thickness higher than 300 μm. To measure the shrinkage we only need the positon of the diffraction peaks. Using these data, we report in Table 6 the values of the shrinkage measured as a function of the recording time for the experimental conditions described in Section 3. As it can be seen in this table, the shrinkage is almost three times bigger in this material than the obtained for PVA/AA. Additionally, for BIO materials the repeatability is slightly lower than that for PVA/AA, therefore the error to determine the shrinkage is now 0.2%. Firstly, we detected a clearly higher value of shrinkage in this photopolymer almost three times the obtained with PVA/AA, more than expected, an so huge to be used as high density holographic data storage medium, in order to improve this drawback the inclusion of nanoparticles can reduce the shrinkage. Additionally, it is important to remark that for

Optical Materials EXPRESS

Biophotopol, Kx increases with the recording time, which can happen due to the high values of shrinkage. One of the possible explanations of this high shrinkage is the high concentration of PVA required to support this thick layers. Elevated concentrations of PVA imply important quantities of water retained by PVA, small portion of this water can be evaporated due to the exothermic chemical reaction during polymerization [28].

Table 6. Measured shrinkage using method 1 for Biophotopol.

Recording time (s)	% Shrinkage Method 1 ± 0.2	Kx (μm^{-1}) ± 0.01
3	0.7	7.33
5	0.8	7.34
8	1.4	7.34
15	2.0	7.37
20	2.6	7.37
30	2.8	7.36
40	3.2	7.37
60	3.5	7.38
80	3.5	7.40

Additionally, for these thick layers is very complicated to measure the DE at the Bragg's angle. Smalls deviation in the Bragg's condition change dramatically the DE measured [30,31]. Therefore, to obtain the maximum DE as a function of time we have recorded many gratings with different recording times. Later, we analyzed the angular responses to obtain the maximum DE. We show these results in Fig. 4 for the diffracted order placed around the angle 7.2° in air. There we show how the maximum DE is obtained very fast between 15 and 20 s of recording time and the DE is very close to the maximum.

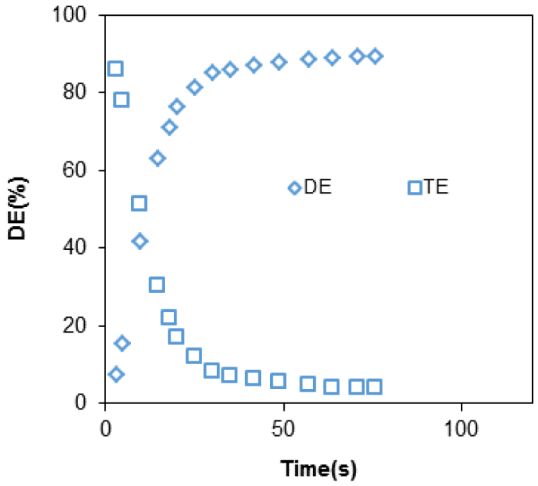

Fig. 4. Max DE as function of recording time for Biophotopol photopolymer 300 µm thick for the diffracted order + 1.

4.3. H-DPLC photopolymer

One of the most attractive properties of HDPLC holograms is the possibility to change the refractive index modulation just applying an electric field to tilt the liquid crystal molecules confined in the dark zones due to the PIPs effect [29]. The magnitude of the electric field applied is directly related to the layer thickness, the thicker is the layer the larger must be the amplitude of the electric field. Therefore, the small modification of the Bragg's condition does not affect so hard to the measured DE at the initial Bragg's angle. The DE as a function of the recording time for HPDLC layers is presented in Fig. 5. It is possible to see how for this

Optical Materials EXPRESS

material also high values of DE, above 80%, can be achieved. The shrinkage measured for different exposure times is presented in Table 7. It is worth remarking that for this material the shrinkage is suppressed partially due to the PIPS effect [29], the nanoparticles are confined in the dark zones, and on the other hand due to the multifunctional monomer that causes more compaction in the polymerized zones. From the analysis of Table 7 we observed a shrinkage close to that of the PVA/AA materials, nevertheless the variation of the Kx is very weak. In this case, the measuring of the shrinkage using only the Bragg's angle detuning of one of the orders can be applied with clearly lower imprecision. In Fig. 4, we present the DE versus exposure time at Bragg's condition + 1, 3.7° in air, due to the low angular selectivity and the reduced shrinkage the angle deviation does not affect the maximum of DE significantly.

Table 7. Measured shrinkage using method 1 for H-PDLC composition.

Recording time (s)	% Shrinkage Method 1	Kx (μm^{-1}) ± 0.01
15	0.2	6.21
20	0.4	6.19
25	0.5	6.19
30	0.8	6.19
35	1.0	6.19
40	1.2	6.20
60	1.2	6.20
80	1.2	6.20

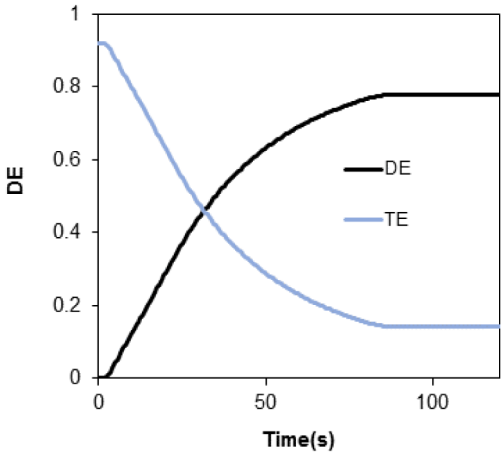

Fig. 5. DE as function of recording time for H-PDLC photopolymer 16 µm thick at Bragg's condition for diffracted order + 1.

4.4. Analysis of the diffracted orders

There are different coupled wave theories, as we commented in the introduction, to reproduce the angular scan of a holographic slanted grating. These are useful to obtain information about the optical thickness, refractive index modulation, absorption and scattering or the attenuation in depth. In addition, as we noted in the introduction the higher orders provide information about the possible deviation from the sinusoidal profile, in the refractive index modulation or thickness. In all the shrinkage models reported in the references [9–18] it is assumed that initially the grating is sinusoidal and after shrinkage remains the same shape of the holographic grating, if during the shrinkage process there are changes in the shape, we expect a-significant variation in the higher diffracted orders. Additionally, in this section, we study the differences between applying Kogelnik wave theory [30], KCW, rigorous coupled wave theory [31], RCW, or time-domain-difference-method [32], TDDM to study the applicability

Optical Materials EXPRESS

of the approximate model of KCW comparing to the rigorous models. It is important to note that the second orders can only be detected for PVA/AA and HPDLC after few seconds of recording and continue growing after the DE of the first one seems stable. This can be explained by saturation in the zones with a maximum of the recording intensity and the remaining chemical reaction in the neighbor zones, in fact this effect was observed also in non-slanted gratings [33] with values of the second harmonic in the refractive index, n_2, around 7 or 8 times smaller than the first one. For the slanted gratings analyzed in this paper, only one of the third diffracted orders are inside of the Ewald's Sphere, nevertheless, in all the cases analyzed is weaker than 0.1% and in the most of them it is very difficult to detect and to fit it with the coupled wave theories. The results for PVA/AA are shown in Table 8, it is important to note that only after 30 s of recording time we can detect the both second diffracted orders, ± 2, even the third, + 3, rarely after 100 s. It is possible also to calculate the value of K using ± 2nd orders. We have checked that the value of Kx calculated from these measurements agree with the obtained from orders ± 1 and we observe the compatibility of both measurements. Comparing the values of DE with the obtained for non-slanted gratings we checked that they are similar, therefore the deviations from the sinusoidal profile do not change for slanted gratings.

Table 8. Measured angles in air for second diffracted orders and their average DE.

Recording time (s)	Angle order + 2 (°) ± 0.002	Angle order –2 (°) ± 0.002	Max DE 2^n order ± 0. 2%
30	23.438	–54.966	0.2%
40	23.319	–55.050	0.4%
60	23.479	–55.399	0.7%
80	23.457	–55.314	1.0%

In Fig. 6.a we depicted the experimental angular scan around the + 1 Bragg's condition for a hologram recorded in PVA/AA material with 40 s of recording time and the fitted simulations provided by KCW and RCW. We show the high agreement between the approximated and rigorous methods. The values obtained from the fitting are: d = 75 μm, n_1 = 0.00325, α = 0.0005 μm^{-1} where d is the thickness, n_1 the first harmonic of the refractive index, and α the coefficient of absorption and scattering. One of the second orders observed after 100 s of recording time is depicted in Fig. 6.b. In this case the experimental data were fitted using RCW, these higher orders are neglected by KCW, the data extracted from this grating were d = 58 μm, n_1 = 0.0032, n_2 = 0.00028, α = 0.003 μm^{-1}, where n_2 is the second harmonic of the refractive index.

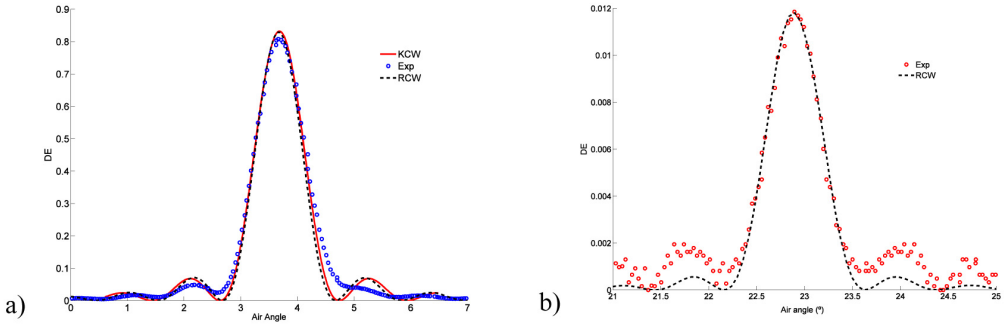

Fig. 6. a) Angular response of diffracted order + 1 for a transmission grating recorded in PVA/AA, experimental data and fittings reported by KCW and RCW. b) Angular response of diffracted order + 2 for a transmission grating recorded in PVA/AA, experimental data and fitting reported RCW.

Optical Materials EXPRESS

For Biophotopol we have not detected any higher diffracted order. Furthermore, we cannot apply the algorithm proposed by Moharam and Gaylor in [31] due to the instabilities generated for large thicknesses. Nevertheless, to validate KCW for these thick slanted gratings, we can use FDTDM [32]. This method was implemented by some authors to optimize the computing time [32]. The results are presented in Fig. 7 and we observe good agreement between experimental data and both electromagnetic methods. The values obtained from the fitting are: d = 285 μm, n_1 = 0.0013, α = 0.0005 μm^{-1}, it is important to note that for this high thickness the value of absorption and scattering coefficient reduces around 13% the DE, due to the high value of the thickness.

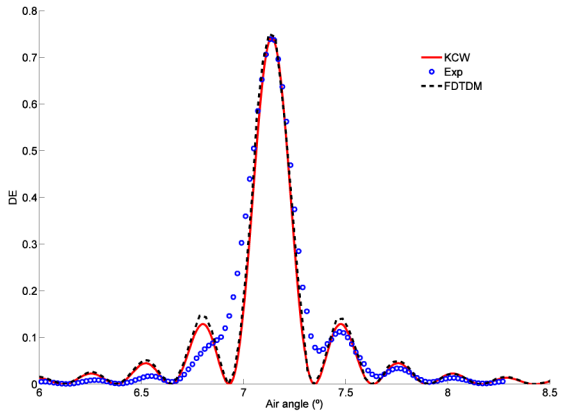

Fig. 7. Angular response of diffracted order + 1 for a transmission grating recorded in Biophotopol, experimental data and fittings reported by KCW and FDTDM.

On the last place, we have studied the higher diffracted order for the photopolymer with dispersed liquid crystal molecules. It is worth noting that in this case we can fit the angular response with RCW. The results for one of the stored gratings are presented in Fig. 8.a. The values obtained from the fitting are: d = 16 μm, n_1 = 0.0115, α = 0.0006 μm^{-1}, but in this case due to the low thickness and the high value of the refractive index modulation we observe small deviation of the approximate model KCW respect to the RCW, this is an expected result predicted in [31]. Concerning to the dimensional and shape changes in the diffraction gratings it is important to note the huge second orders detected for these slanted gratings. For the same grating we have measured the second order in Fig. 8.b, and as it can be seen, the DE achieved a value close to 20%, we fitted this experimental data with RCW and where d = 15.5 μm, n_2 = 0.0065, α = 0.0006 μm^{-1}. We have checked this value with the obtained with non-slanted gratings and they have similar size. Maybe these higher harmonics are due to the high functionality of monomer and crosslinker in HPDLC systems [29], in this case one of the third harmonics can be detected with efficiencies around 1%, or due to the PIPs effect.

Optical Materials EXPRESS

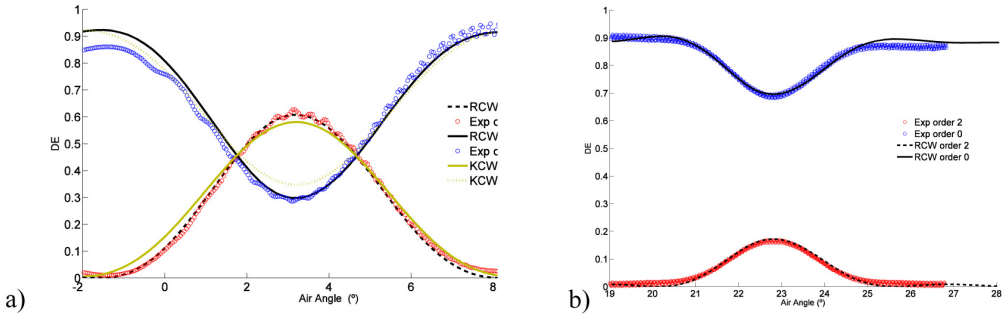

Fig. 8. a). Angular response of diffracted order + 1 for a transmission grating recorded in HPDLC, experimental data and fittings reported by KCW and RCW. b) Angular response of diffracted order + 2 for a transmission grating recorded in HPDLC, experimental data and fitting reported RCW.

5. Conclusions

Along this work, we have studied the dimensional changes in three different photopolymers. We have detected in two of them, PVA/AA and Biophotopol a clear variation of the component x of the grating vector, this surprising fact makes impossible to apply some of the classical methods to measure the shrinkage consisting in the detuning of the first Bragg's angle. As an alternative, we recommend the mandatory measurement of the Bragg's angles for both orders ± 1, from these data, we can calculate the shrinkage using two different equations with similar results. For the third material, HPDLC, the value of Kx remains almost constant; nevertheless, for these metrology measurements, where high precision is required, we suggest also determining shrinkage from the values of both first Bragg's angles. In order to analyze how the shrinkage affects on the grating shape we have measured higher diffracted orders using different electromagnetic theories, we can conclude that the shrinkage does not increase the deformations in the sinusoidal profile significantly.

Acknowledgments

This work was supported by the "Ministerio de Economía y Competitividad" (projects FIS2015-66570-P and FIS2014-56100-C2-1-P) and by the "Generalitat Valenciana" of Spain (projects PROMETEOII/2015/015 and ISIC/2012/013).